OPEN ACCESS
Freely Available Online

JOURNAL OF ADVANCED PHARMACEUTICAL SCIENCE AND TECHNOLOGY
ISSN NO: 2328-0182

Research article

DOI: 10.14302/issn.2328-0182.japst-21-3715

Investigation on the Impact of Biofield Energy Treatment on the Physical, Thermal and Spectroscopic Characteristics of Zinc Chloride

Mahendra Kumar Trivedi[1], Snehasis Jana[2,*]

[1]Trivedi Global, Inc., Henderson, Nevada, USA
[2]Trivedi Science Research Laboratory Pvt. Ltd., Thane (W), Maharashtra, India

Abstract

Zinc is an essential trace mineral that plays an important role in the human body as a regulator for different enzymatic systems. It is used in various supplements in the form of zinc chloride to meet the daily requirements. This study was designed with the aim to investigate the impact of The Trivedi Effect®- Energy of Consciousness Healing Treatment on the various physical, thermal, and spectral properties of zinc chloride. The study involves dividing the zinc chloride sample in two parts, followed by keeping the first part untreated and named it the control sample. Besides, The Trivedi Effect®- Biofield Energy Healing Treatment was provided to the other part remotely by the renowned Biofield Energy Healer, Mr. Mahendra Kumar Trivedi and the sample was termed as Biofield Energy Treated sample. Later on, both the samples were analyzed using PXRD, PSA, DSC, UV-Vis, and FT-IR analytical techniques. The PXRD analysis revealed the significant changes in the crystallite sizes (from -66.68% to 25.02%) and the relative peak intensities (from -81.35% to 141.22%) along with 26.46% decrease in the average crystallite size of the Biofield Energy Treated sample, compared with the control sample. Additionally, the treated sample showed reduction in the particle sizes d_{10}, d_{50}, d_{90}, and D(4,3) values by 92.18%, 23.24%, 14.48%, and 29.31%, respectively as compared to the control sample. However, the surface area of the treated sample was observed to be significantly increased by 224.57%, compared to the control sample. The DSC analysis revealed slight increase in the melting and decomposition temperature of the Biofield Energy Treated sample by 0.84% and 3.62%, respectively; along with the significant increase in the latent heat of melting and decomposition by 24.85% and 123.23%, respectively, compared to the control sample. It showed that the thermal stability of the treated sample was significantly increased. However, the UV-Vis and FT-IR studies revealed that the structural properties of the control and treated samples were remained same. The overall study represents that The Trivedi Effect®- Energy of Consciousness Healing Treatment may be used to generate a polymorphic form of zinc chloride, which might possess enhanced solubility, dissolution and bioavailability profile along with improved thermal stability, compared to the control sample. Such properties of the treated zinc chloride may ensure its efficacy, stability and safety during the process of shipment, handling, and storage; thus, The Trivedi Effect®-Energy of Consciousness Healing Treated zinc chloride would be useful for designing the better formulation with enhanced bioavailability, stability and efficacy profile.

OPEN ACCESS
Freely Available Online

OpenAccessPub

Corresponding author: Snehasis Jana, Trivedi Science Research Laboratory Pvt. Ltd., Thane (W), Maharashtra, India, Tel: +91- 022-25811234
Citation: Mahendra Kumar Trivedi, Synthesis Jana (2021) Investigation on the Impact of Biofield Energy Treatment on the Physical, Thermal and Spectroscopic Characteristics of Zinc Chloride. Journal of Advanced Pharmaceutical Science And Technology - 2(4):11-25. https://doi.org/10.14302/issn.2328-0182.japst-21-3715

Keywords: Zinc chloride, The Trivedi Effect®, Energy of Consciousness Healing Treatment, PXRD, Particle size, DSC, FT-IR

Received: Jan 19, 2021 **Accepted:** Feb 04, 2021 **Published:** Feb 10, 2021

Editor: Fatma Mohammed Mady, Department of Pharmaceutics, Minia University, Egypt.

Introduction

Zinc is the essential trace element required in very less amount for the healthy human body. However, it is the only metal present in the enzyme classes and the most abundant mineral ion after magnesium in the human body [1]. Zinc is required for the functioning of those enzymes that are involved in the metabolism of the carbohydrates, proteins and fats. Besides, it is also involved in maintaining the normal serum testosterone concentrations, balancing the different forms of prostaglandins, and thus plays important role in fertility and reproduction [2]. It is also used in the treatment of recurrent ear infections, common cold and for enhancing the immune system, thereby preventing the lower respiratory tract infections. Moreover, the zinc supplements are used for the treatment as well as prevention of the deficiency disorders such as, acute diarrhoea and retarded growth in the children as well as slow wound healing. [3]. The use of zinc is also evident in the treatment of diabetes, asthma, acquired immunodeficiency syndrome (AIDS), hypertension, and some skin conditions such as eczema, psoriasis, and acne. Sometimes, the people use it in the treatment of some eye disorders such as the macular degeneration caused in night blindness and cataracts. Also, it is used for the parasitic diseases such as malaria [4, 5]. Apart from that, the other uses of zinc include the treatment of hypogeusia, attention deficit-hyperactivity disorder (ADHD), severe head injuries, ringing in the ears (tinnitus), Alzheimer's disease, Hansen's disease, Crohn's disease, peptic ulcers, Wilson's disease, Down syndrome, and ulcerative colitis [6]. The other diseases involving the use of zinc for treatment are male infertility, benign prostatic hyperplasia (BPH), osteoporosis, acrodermatitis, erectile dysfunction (ED), rheumatoid arthritis, thalassemia, and muscle cramps due to the liver disease [7-10]. The zinc supplements are also used by some athletes for improving their strength and athletic performance. Besides, it is also proved to be useful for herpes simplex infections, aging skin, and wound healing [11].

The food is good source of zinc; however, the body can only absorb 20-40% from it. Also, the bioavailability is twice higher from the animal sources in terms of absorption rather than from the plant sources. Moreover, the rate of absorption is higher if zinc is taken with the protein meal, but still the body is unable to store it for the long term uses. Thus, it is needed to supplement the zinc in small quantities every day. There were several reports that compare the bioavailability of different forms of zinc in the humans and it was reported that zinc chloride is a good source among them [12]. The absorption route of zinc in human body involves its dissociation in the form of ions that further bind to the ligands for getting transported into the cells of the small intestine. Later on, the intestinal linings possess specific transport proteins, which help in carrying the zinc into the circulation, across the cell membrane. From there, the zinc ions are transported directly to the liver for getting delivered to all the tissues. Thus, nearly 70% of zinc is present in the bounded state to the serum albumin and fewer amounts are freely available in the circulation for the need of body [13]. In this regard, the current study was designed to improve the bioavailability of the zinc chloride by using the approach of Biofield Energy Treatment. The Biofield Energy Healing Treatment is known for its considerable impact on the properties of

drug molecules such as, particle size, surface area, and thermal behaviour, etc. through possible mediation of neutrinos [14-16]. It is a type of unique energy in the form of electromagnetic field surrounding the human body, which is infinite and para-dimensional. Such kind of Biofield (Putative Energy Fields) based Energy Healing Therapies have been also known for their useful outcomes against the treatment of various diseases [17]. Thus, the National Institute of Health/ National Center for Complementary and Alternative Medicine (NIH/NCCAM) has been included such Energy therapy under the category of Complementary and Alternative Medicine (CAM) and it is now widely accepted by the U.S. population [18]. In this regard, the Trivedi Effect®-Consciousness Energy Healing Treatment has also been widely reported for its impact on the physicochemical properties of pharmaceutical products [19, 20], metals, ceramics, polymers, and organic compounds [21-23], nutraceuticals [24, 25], and its impact in agricultural science [26, 27], livestock [28], and skin health [29, 30]. The recent studies reported the impact of The Trivedi Effect®-Consciousness Energy Healing Treatment in decreasing the particle size and improving the surface area of pharmaceutical/nutraceutical compounds, which might prove to be advantageous in enhancing the bioavailability profile of the drug [31, 32]. Thus, this study was designed to analyze the effect of the Biofield Energy Healing Treatment (The Trivedi Effect®) on the physicochemical, thermal and spectral properties of zinc chloride by using the techniques of PXRD, PSD, DSC, UV-vis spectroscopy, and FT-IR spectrometry.

Materials and Methods

Chemicals and Reagents

Zinc chloride was procured from Tokyo Chemical Industry Co., Ltd. (TCI), Japan. All other chemicals used in the experiment were of analytical grade available in India.

Consciousness Energy Healing Treatment Strategies

The study involves zinc chloride as the test compound, which was divided into two parts and named as the control and treated sample. Among them, the control part did not receive the Biofield Energy Treatment; whereas, the treated part of the test compound was given the Energy of Consciousness Healing Treatment by the renowned Biofield Energy Healer, Mr. Mahendra Kumar Trivedi (USA), and further labelled as the Biofield Energy Treated zinc chloride. In the process of Biofield Energy Treatment, the sample was placed under the standard laboratory conditions and the Healer remotely provided the Trivedi Effect® - Energy of Consciousness Healing Treatment to the sample for 3 minutes with the help of the Unique Energy Transmission process. Nevertheless, the control sample was subjected to "sham" healer under the similar laboratory conditions, who did not have any knowledge about the Biofield Energy Treatment. Later on, both the samples were kept in similar sealed conditions and further characterized using PXRD, PSA, DSC, UV-Vis, and FTIR analytical techniques.

Characterization

Powder X-ray Diffraction (PXRD) Analysis

The PXRD analysis of zinc chloride was done using PANalytical X'Pert3 powder X-ray diffractometer, UK. The copper line was used as the source of radiation for diffraction of the analyte at 0.154 nm X-ray wavelength that is running at 40 mA current and 45 kV voltage. Moreover, the instrument uses a scanning rate of 18.87°/second over a 2q range of 3-90° and the ratio of Kα-2 and Kα-1 was 0.5 (k, equipment constant). The data was collected using X'Pert data collector and X'Pert high score plus processing software in the form of a chart of the Bragg angle (2θ) *vs.* intensity (counts per second), and a detailed table containing information on peak intensity counts, d value (Å), full width half maximum (FWHM) (°2θ), relative intensity (%), and area (cts*°2θ). The crystallite size (G) was calculated by using the Scherrer equation (1) as follows:

$$G = k\lambda/(b\cos\theta) \quad (1)$$

Where, k is the equipment constant (0.5), λ is the X-ray wavelength (0.154 nm); b in radians is the full-width at half of the peaks and θ is the corresponding Bragg angle.

Percent change in crystallite size (G) of zinc chloride was calculated using following equation 2:

$$\%\ \text{change in crystallite size} = \frac{[G_{\text{Treated}} - G_{\text{Control}}]}{G_{\text{Control}}} \times 100 \quad ...(2)$$

Where, $G_{Control}$ and $G_{Treated}$ are the crystallite size of the control and Biofield Energy Treated zinc chloride samples, respectively.

Particle Size Analysis (PSA)

The particle size analysis of the samples were done using wet method, which is conducted on Malvern Mastersizer 3000, UK with a detection range between 0.01 µm to 3000 µm [31]. In this method, the sample unit (Hydro MV) was filled with light liquid paraffin oil (act as dispersant medium) and stirred at 2500 rpm. The refractive index values for dispersant medium and samples were 0.0 and 1.47, respectively. The measurement was taken twice after reaching obscuration in between 10% and 20%, followed by averaging the two measurements. The analysis shows d (0.1) µm, d(0.5) µm, d(0.9) µm values that represent the particle diameter corresponding to 10%, 50%, and 90% of the cumulative distribution. The calculations were done by using software Mastersizer V3.50.

The percent change in particle size (d) for d_{10}, d_{50} and d_{90} was calculated using following equation 3:

$$\% \text{ change in particle size} = \frac{[d_{Treated} - d_{Control}]}{d_{Control}} \times 100 \quad \text{.....(3)}$$

Where, $d_{Control}$ and $d_{Treated}$ are the particle size (µm) for at below 10% level (d_{10}), 50% level (d_{50}), and 90% level (d_{90}) of the control and Biofield Energy Treated samples, respectively.

Percent change in surface area (S) was calculated using following equation 4:

$$\% \text{ change in surface area} = \frac{[S_{Treated} - S_{Control}]}{S_{Control}} \times 100 \quad \text{.....(4)}$$

Where, $S_{Control}$ and $S_{Treated}$ are the surface area of the control and Biofield Energy treated zinc chloride, respectively.

Differential Scanning Calorimetry (DSC)

The DSC analysis of the samples was performed using DSC Q2000 differential scanning calorimeter, USA under the dynamic nitrogen atmosphere with flow rate of 50 mL/min. It includes a sample mass of ~2.5 mg using aluminum pan which is heated at the rate of 10 ºC/min from 30 °C to 450 °C [32]. Later on, the percent change in melting point (T) of the control and treated samples was calculated using following equation 5:

$$\% \text{ change in melting point} = \frac{[T_{Treated} - T_{Control}]}{T_{Control}} \times 100 \quad \text{....(5)}$$

Where, $T_{Control}$ and $T_{Treated}$ are the melting point of the control and treated zinc chloride samples, respectively.

Also, the percent change in the latent heat of fusion (ΔH) was calculated using following equation 6:

$$\% \text{ change in latent heat of fusion} = \frac{[\Delta H_{Treated} - \Delta H_{Control}]}{\Delta H_{Control}} \times 100 \quad \text{.....(6)}$$

Where, $\Delta H_{Control}$ and $\Delta H_{Treated}$ are the latent heat of fusion of the control and treated zinc chloride, respectively.

Ultraviolet-visible Spectroscopy (UV-Vis) Analysis

The UV-Vis spectral analysis of the control and treated zinc chloride samples were carried out using Shimadzu UV-2400PC SERIES with UV Probe (Shimadzu, JAPAN). The spectrum was recorded in the wavelength range of 190-800 nm using 1 cm quartz cell that has a slit width of 0.5 nm. The absorbance spectra (in the range of 0.2 to 0.9) and wavelength of maximum absorbance (λ_{max}) were recorded.

Fourier Transform Infrared (FT-IR) Spectroscopy

FT-IR spectroscopy of zinc chloride was performed on Spectrum ES Fourier transform infrared spectrometer (Perkin Elmer, USA) by using pressed KBr disk technique with the frequency array of 400-4000 cm^{-1}. The technique uses ~2 mg of control sample and about 300 mg of KBr as the diluent to form the pressed disk followed by running the sample in the spectrometer. The same procedure was adopted for the Biofield Energy Treated sample.

Results and Discussion

Powder X-ray Diffraction (PXRD) Analysis

The PXRD diffractograms of the control and Biofield Energy Treated samples of zinc chloride are shown in Figure 1. There are the sharp and intense peaks in the diffractograms of both the samples, which represents that both the samples are crystalline in nature. Moreover, the data of PXRD analysis is

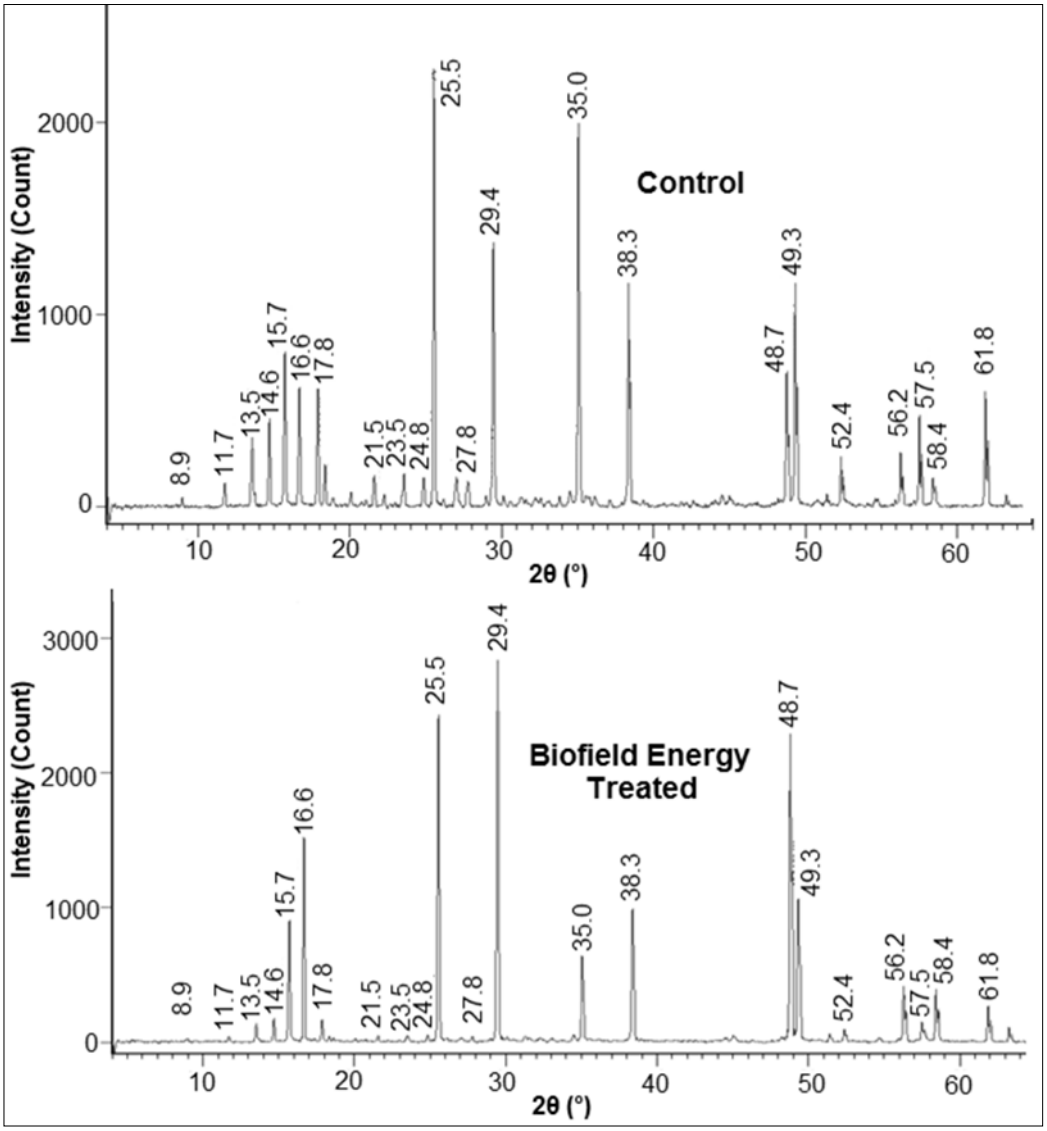

Figure 1. PXRD diffractograms of the control and Biofield Energy Treated zinc chloride.

presented in Table 1 that includes the Bragg angle (2θ), relative peak intensity (%), and crystallite size (G) for both the samples*, i.e.,* the control and Biofield Energy Treated zinc chloride. During the analysis, the crystallite size was calculated with the help of Scherer equation [33].

The analysis revealed that the crystallite sizes of the Biofield Energy Treated sample at 2θ equal to nearly 11.7°, 21.5°, and 24.8° (Table 1, entry 2, 8, and 10) was increased by 25.02, 8.34, and 20.02%, respectively as compared to the control sample. Although, the crystallite sizes at 2θ equal to nearly 16.6°, 17.8°, and 57.5° (Table 1, entry 6, 7, and 19) of the Biofield Energy Treated zinc chloride didn't showed any alteration, compared with the control sample; however, the crystallite sizes at remaining 2θ (Table 1, entry 1, 3-5, 9, 11-18, 20, and 21) of the treated sample were significantly decreased in the range from 12.50% to 66.68%, as compared to the control sample. Additionally, the average crystallite sizes of the Biofield Energy Treated zinc chloride was calculated as 32.71 nm, which was significantly reduced by 26.46% as compared to the control sample (44.48 nm). Besides, the PXRD diffractogram revealed the highest peak intensity (100%) of both the samples, in which the control sample showed the peak at Bragg's angle (2θ) equal to 25.5° (Table 1, entry 11), whereas, the Biofield Energy Treated zinc chloride showed the peak at 29.4° (Table 1, entry 12). Moreover, the other peaks of Biofield Energy Treated sample's diffractogram showed significant alterations in their relative peak intensities in the range from -81.35% to 141.22%, compared to the control sample. Some studies reported that the alterations in the relative intensity of the crystalline compound may depend on the crystal morphology [34]. Thus, it is presumed that the Biofield Energy Healing Treatment probably transfer the energy within the sample that might altered the crystal morphology, which ultimately resulted in the altered crystallinity and crystallite size of the Biofield Energy Treated sample as compared to the control sample. Besides, such alterations in the XRD pattern of the crystalline compound may also be considered as the sign of polymorphic transitions [35, 36]. Hence, it is presumed that the Biofield Energy Treatment might produces a new polymorphic form of zinc chloride that may affects the solubility, dissolution, and bioavailability parameters of the drug [37].

Particle Size Analysis (PSA)

The particle size and surface area of the control and Biofield Energy Treated zinc chloride were presented and analyzed in Table 2. The study showed that the particle sizes at d_{10}, d_{50}, d_{90}, and D(4,3) of the control sample were observed as 51.18µm, 150.99µm, 255.53µm, and 152.79µm, respectively. Consequently, the particle size distribution of the Biofield Energy Treated sample at d_{10}, d_{50}, d_{90}, and D(4,3) was found as 4.00µm, 115.90µm, 218.52µm, and 108.0µm, respectively. The analysis revealed that in the Biofield Energy Treated zinc chloride, the particle size values at d_{10}, d_{50}, d_{90}, and D(4,3) was significantly decreased by 92.18%, 23.24%, 14.48%, and 29.31%, respectively as compared with the control sample. However, the specific surface area (SSA) of Biofield Energy Treated zinc chloride (435.90m^2/Kg) was significantly increased by 224.57% with respect to the control sample (134.30m^2/Kg).

It is presumed that the Biofield Energy Treatment might cause the decreased particle size by probably fracturing the internal boundaries of particles and thereby resulted into the particles of smaller size [38]. Later on, the increased surface area of Biofield Energy Treated sample might happen due to this decrease in particle size as compared to the control sample [39]. The particle size and surface area plays important role in the dissolution and bioavailability profile of the drug [40]. The surface area is vital parameter as it affects the surface energy, which is the driving factor in terms of the dissolution efficiency along with the chemical affinity [41]. Hence, it could be concluded that the Biofield Energy Treatment might help in enhancing the solubility, dissolution and absorption rate and the bioavailability of the zinc chloride.

Differential Scanning Calorimetry (DSC) Analysis

The DSC thermograms of the control and Biofield Energy Treated zinc chloride are presented in Figure 2. Also, the melting temperature and enthalpy of fusion of the control and Biofield Energy Treated zinc chloride are analyzed and presented in the Table 3. The

Table 1. PXRD data for the control and Biofield Energy Treated zinc chloride.

Entry No.	Bragg angle (°2q)	Relative Peak Intensity (%)			Crystallite size (G, nm)		
		Control	Treated	% change [a]	Control	Treated	% change [b]
1	8.9	2.24	0.72	-67.86	43.15	14.38	-66.68
2	11.7	5.89	1.52	-74.19	34.59	43.25	25.02
3	13.5	16.97	4.84	-71.48	43.33	34.65	-20.02
4	14.6	21.56	6.42	-70.22	43.38	31.54	-27.29
5	15.7	37.77	32.33	-14.40	34.74	28.95	-16.68
6	16.6	28.66	54.49	90.13	31.61	31.61	0.00
7	17.8	28.66	5.96	-79.20	34.83	34.83	0.00
8	21.5	7.77	1.53	-80.31	26.94	29.19	8.34
9	23.5	7.99	1.49	-81.35	35.15	19.52	-44.46
10	24.8	7.13	1.73	-75.74	29.36	35.24	20.02
11	25.5	100.0	86.43	-13.57	44.12	29.40	-33.36
12	29.4	62.33	100.0	60.44	44.49	27.37	-38.48
13	35.0	91.63	20.72	-77.39	72.13	30.07	-58.31
14	38.3	54.32	33.97	-37.46	59.75	33.12	-44.56
15	48.7	33.02	79.65	141.22	44.26	38.73	-12.50
16	49.3	54.58	37.46	-31.37	51.76	34.51	-33.33
17	52.4	12.09	2.66	-78.00	52.44	19.66	-62.50
18	56.2	13.2	14.65	10.98	53.34	35.56	-33.33
19	57.5	22.32	5.13	-77.02	53.67	53.67	0.00
20	58.4	6.86	13.95	103.35	53.91	40.43	-25.00
21	61.8	28.07	9.44	-66.37	47.01	41.14	-12.50

[a]denotes the percentage change in the relative intensity of Biofield Energy Treated sample with respect to the control sample; [b]denotes the percentage change in the crystallite size of Biofield Energy Treated sample with respect to the control sample.

Table 2. Particle size distribution of the control and Biofield Energy Treated zinc chloride

Test Item	**d_{10} (µm)**	**d_{50} (µm)**	**d_{90} (µm)**	**D(4,3) (µm)**	**SSA(m^2/Kg)**
Control sample	51.18	150.99	255.53	152.79	134.30
Biofield Energy Treated sample	4.00	115.90	218.52	108.0	435.90
Percent change* (%)	-92.18	-23.24	-14.48	-29.31	224.57

d_{10}, d_{50}, and d_{90}: particle diameter corresponding to 10%, 50%, and 90% of the cumulative distribution, D (4,3) : the average mass-volume diameter, SSA : the specific surface area; *denotes the percentage change in the particle size distribution of the Biofield Energy Treated sample with respect to the control sample.

Table 3. The latent heat of fusion (J/G) and melting point (°C) values of the control and Biofield Energy Treated zinc chloride.

Peak	Description	T_{onset} (°C)	T_{peak} (°C)	T_{endset} (°C)	ΔH (J/g)
Endothermic peak	Control sample	292.87	306.26	317.61	565.1
	Biofield Treated sample	295.21	308.83	317.61	705.5
	% Change*	0.80	0.84	0.00	24.85
Exothermic peak	Control sample	381.75	383.81	390.55	1016
	Biofield Treated sample	382.80	397.71	396.53	2268
	% Change*	0.28	3.62	1.53	123.23

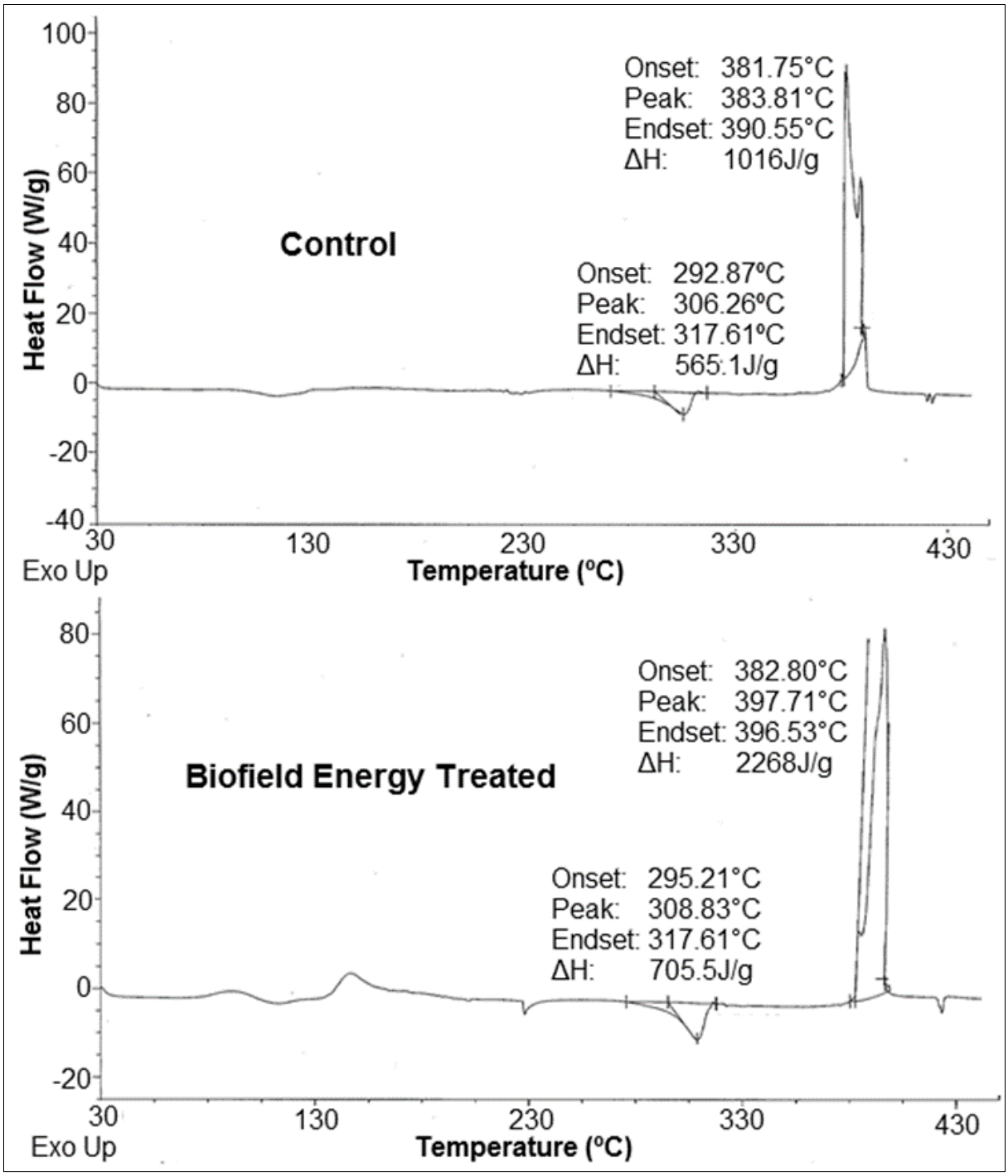

Figure 2. DSC thermograms of the control and Biofield Energy Treated zinc chloride.

melting/fusion temperature in the treated zinc chloride was observed at 308.83°C which was slightly increased by 0.84% as compared to the control sample (306.26° C). The onset melting temperature of the Biofield Energy Treated sample was also slightly increased by 0.80% compared with the control sample. The enthalpy of fusion (ΔH_{fusion}) of the control and Biofield Energy Treated zinc chloride was 565.10J/g and 705.5J/g, respectively. The ΔH_{fusion} of the Biofield Energy Treated sample was significantly increased by 24.85% compared with the control sample. Besides, the decomposition temperature of the Biofield Energy Treated zinc chloride was observed at 397.71°C, as compared to the control sample at 383.81°C, thus showed the increase by 3.62%. Also, the onset and endset decomposition temperatures of the Biofield Energy Treated sample showed slight increase by 0.28% and 1.53%, respectively, compared with the control sample.

Nevertheless, the enthalpy of decomposition ($\Delta H_{decomposition}$) of the control and Biofield Energy Treated zinc chloride were observed as 1016J/g and 2268 J/g, respectively. It showed that the $\Delta H_{decomposition}$ of the Biofield Energy Treated sample was significantly increased by 123.23% compared with the control sample. In a solid, the latent heat of fusion (ΔH) is considered as the energy that is needed to overcome the interaction forces, which are responsible for holding the atoms of the solid at their positions and thereby converting it in the form of liquid [42]. In the Biofield Energy Treated sample, there is the considerable increase in ΔH, which revealed that the treated sample needs more energy to undergo the process, as compared to the control sample. The overall thermal study indicated the increase in thermal stability of the Biofield Energy Treated sample, as compared to the control sample that may help in the stability, long term storage and shipping of the zinc chloride [43].

Ultraviolet-visible Spectroscopy (UV-Vis) Analysis

The UV-visible spectra of the control and Biofield Energy Treated zinc chloride samples are presented in Figure 3.

The UV-Vis spectra showed that both the control and Biofield Energy Treated samples possess the wavelength of the most intense UV-Vis absorbance (λ_{max}) at 196.0 nm (Figure 3). However, the absorbance maxima was slightly altered from 2.2740 (control) to 2.2989 in the Biofield Energy Treated sample. The UV absorbance and thereby the UV-Vis spectra occurred as a result of the excitation of electrons from highest energy occupied molecular orbital (HOMO) to lowest energy unoccupied molecular orbital (LUMO) [44]. However, the spectral analysis revealed no change in the λ_{max} of the Biofield Energy Treated sample as compared to the control. It revealed that the energy gap between the HOMO and LUMO and the structural configuration in the Biofield Energy Treated sample was similar as that of the control sample.

Fourier Transform Infrared (FT-IR) Spectroscopy

The FT-IR spectra of the control and Biofield Energy Treated samples of zinc chloride are presented in the Figure 4.

Zinc (II) chloride is a tri-atomic molecule and is linear with four numbers of normal modes of vibration. However, there might be some peaks in the FT-IR spectra due to the O-H stretching because of the presence of zinc chloride hydrates $\{ZnCl_2(H_2O)n$ where n = 1, 1.5, 2.5, 3, and 4$\}$. The FT-IR spectrum of the control sample showed strong absorption band at 3589 cm^{-1}, 3517 cm^{-1} (O-H stretching) and at 1606 cm^{-1} (H-O -H bending) , which denoted that there might be presence of the lattice water (Figure 4). Consequently, in the spectrum of the Biofield Energy Treated zinc chloride, the peaks for the lattice water were observed at 3588, 3518, and 1607 cm^{-1}. Moreover, according to the literature, the metal stretching absorption band was found in the frequency region 750-1000 cm^{-1} in case of the inorganic materials [45]. Thus, in the spectrum of the control sample, this metal-halogen (Zn-Cl) stretching peak was observed at 511 cm^{-1}, whereas in the Biofield Energy Treated sample, it was observed at 513 cm^{-1}. Also, there were some additional peaks in the region of 650-1000 cm^{-1}. Overall, the FT-IR spectra of both the control and Biofield Energy Treated samples of zinc chloride showed similar pattern in both the functional group and fingerprint region, thereby concluded no structural modification.

Conclusions

The overall study concluded the significant

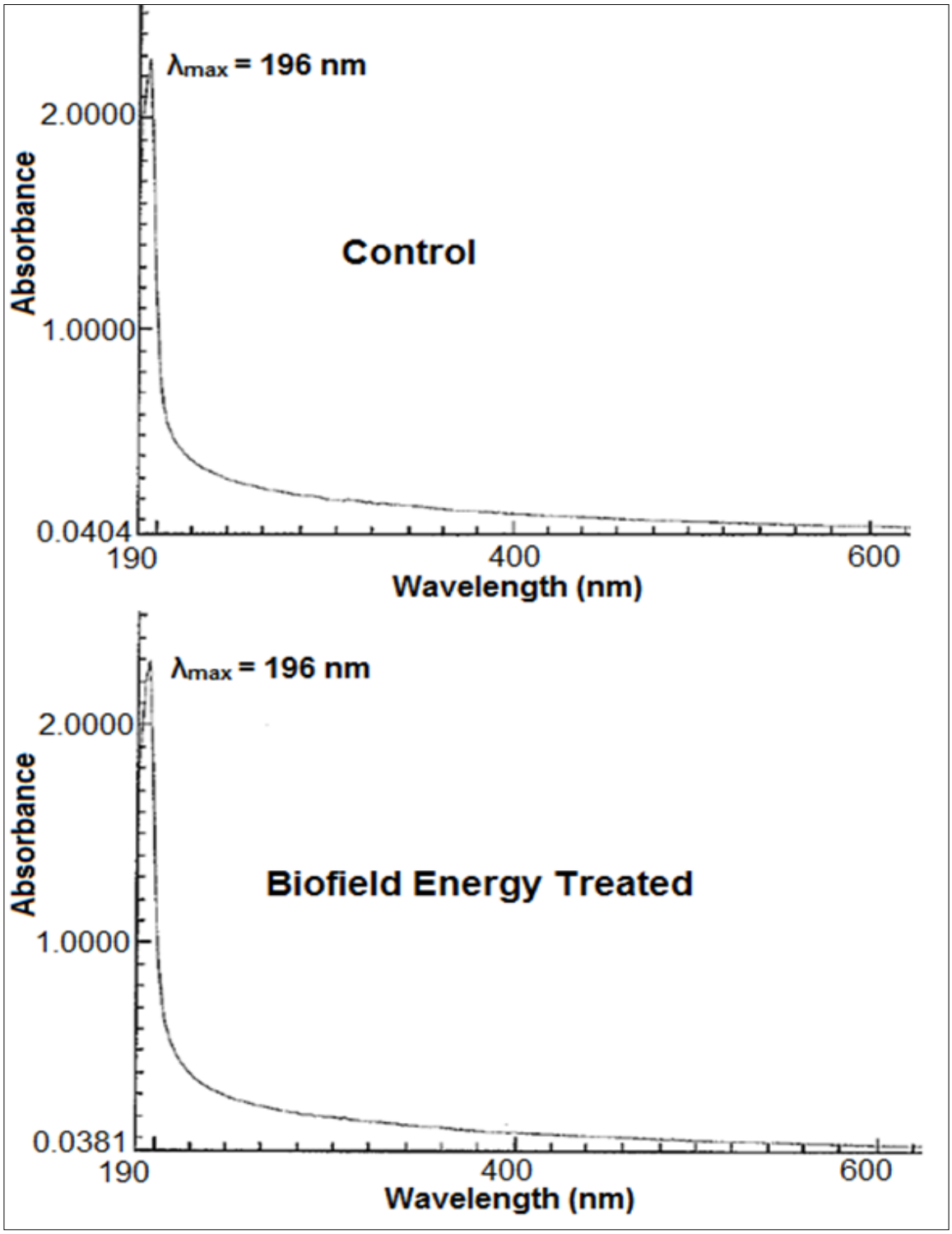

Figure 3. UV-vis spectra of the control and Biofield Energy Treated zinc chloride.

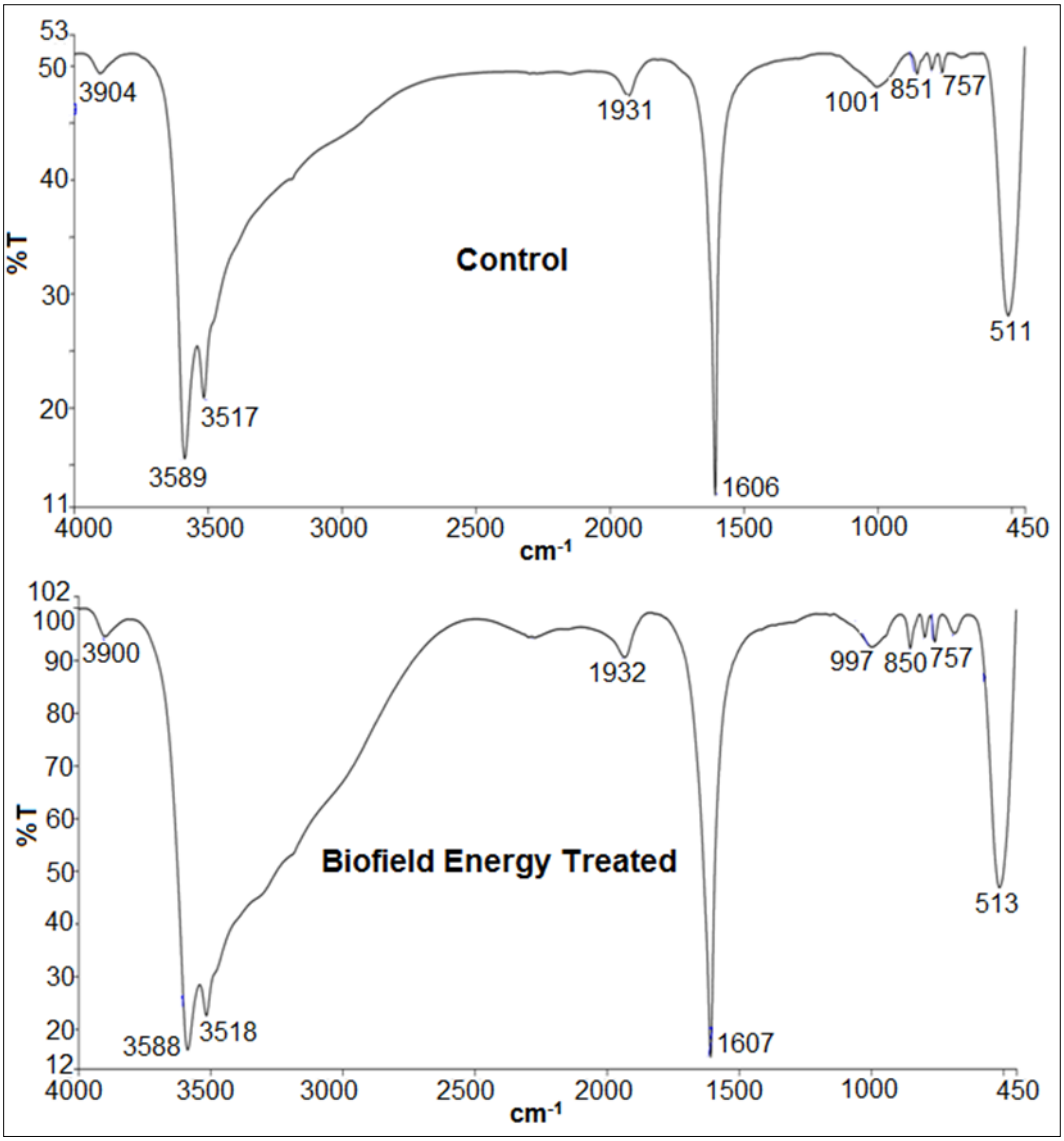

Figure 4. FT-IR spectra of the control and Biofield Energy Treated zinc chloride.

impact of The Trivedi Effect®- Energy of Consciousness Healing Treatment on the physical and thermal properties of zinc chloride. The PXRD study reported that after the Biofield Energy Treatment, the treated zinc chloride sample showed alterations in the relative peak intensities of the characteristic peaks in the range from -81.35% to 141.22%, compared to the control sample. Also, the highest peak intensity (100%) was observed at 2θ equal to 29.4° in the Biofield Energy Treated sample, instead of 25.5° as shown in the diffractogram of the control sample. Besides, the crystallite sizes across the plane of the characteristic peaks were also found to be altered in the Biofield Energy Treated sample in the range -66.68% to 25.02%, along with 26.46% reduction in the average crystallite size, compared with the control sample. Such alterations in the relative peak intensities and crystallite size of the Biofield Energy Treated zinc chloride indicated the changes in the crystallinity and the regular pattern of the atoms and might suggest the presence of a new polymorphic form of compound. Later on, the particle size analysis showed a significant reduction in the values of d_{10}, d_{50}, d_{90}, and D(4,3) of the Biofield Energy Treated sample by 92.18%, 23.24%, 14.48%, and 29.31%, respectively as compared to the control sample. However, the surface area of the treated sample was observed to be significantly enhanced by 224.57% compared to the control sample. Such changes may occur after the Biofield Energy Treatment of the sample, which might cause the fracturing of the internal boundaries of particles and resulted into the smaller sized particles with the increased surface area of the treated zinc chloride sample. Nevertheless, the melting and decomposition temperatures of the Biofield Energy Treated sample were slightly increased by 0.84% and 3.62%, respectively, whereas, the ΔH_{fusion} and $\Delta H_{decomposition}$ were significantly increased by 24.85% and 123.23%, respectively, compared to the control sample. It suggests that the thermal stability of the Biofield Energy Treated zinc chloride sample was increased after the Biofield Energy Treatment. Overall, the study showed the significant impact of The Trivedi Effect®-The Energy of Consciousness Healing Treatment on the physical and thermal properties of zinc chloride, which might produce a new polymorphic form of the zinc chloride sample along with reduced crystallite and particle size and increased surface area. Such altered properties may help in enhancing the solubility, dissolution, absorption, and bioavailability profile of The Trivedi Effect® Treated zinc chloride. Also, the Energy of Consciousness Healing Treatment might help in enhancing the thermal stability that further useful in designing a better nutraceutical and/or pharmaceutical formulations with enhanced bioavailability, stability and safety profile. Hence, the Energy of Consciousness Healing Treatment may help in providing better therapeutic response regarding the treatment of various deficiencies and disorders, such as, hypogeusia, attention deficit-hyperactivity disorder (ADHD), severe head injuries, ringing in the ears (tinnitus), male infertility, benign prostatic hyperplasia (BPH), osteoporosis, acrodermatitis, erectile dysfunction (ED), rheumatoid arthritis, thalassemia, Alzheimer's disease, Hansen's disease, Crohn's disease, peptic ulcers, Wilson's disease, Down syndrome, and ulcerative colitis, etc.

Acknowledgements

The authors are grateful to GVK Biosciences Pvt. Ltd., Trivedi Science, Trivedi Global, Inc., and Trivedi Master Wellness for their assistance and support during this work.

References

1. Prasad AS (1995) Zinc: An overview. Nutrition 11: 93-99.
2. Prasad AS (2008) Clinical, immunological, anti-inflammatory and antioxidant roles of zinc. Exp Gerontol 43: 370-377.
3. Haase H, Rink L (2009) Functional significance of zinc-related signaling pathways in immune cells. Annu Rev Nutr 29: 133-52.
4. Prasad AS (1985) Clinical manifestations of zinc deficiency. Annu Rev Nutr 5: 341-363.
5. Behrens R, Tomkins A, Roy S (1990) Zinc supplementation during diarrhea, a fortification against malnutrition? Lancet 336: 442-443.
6. Hambidge M (2000) Human zinc deficiency. J Nutr 130: 1344S-1349S.
7. Russell RM, Cox ME, Solomons N (1983) Zinc and the special senses. Ann Int Med 99: 227-239.

8. Solomons N (1984) Zinc. In: Clinical guide to parenteral micronutrition, (ed. Baumgartner TG) (1st edn) Educational Publications.
9. Prasad A (1991) Discovery of human zinc deficiency and studies in an experimental human model. Am J Clin Nutr 53: 403-412.
10. Sandstead H (1985) Zinc: Essentiality for brain development and function. Nutr Rev 43: 129-137.
11. Takeda A, Tamano H (2009) Insight into zinc signaling from dietary zinc deficiency. Brain Res Rev 62: 33-44.
12. Maret W, Sandstead HH (2006) Zinc requirements and the risks and benefits of zinc supplementation. J Trace Elem Med Biol 20: 3-18.
13. Vallee BL, Falchuk KH (1993) The biochemical basis of zinc physiology. Physiol Rev 73: 79-118.
14. Trivedi MK, Mohan TRR (2016) Biofield energy signals, energy transmission and neutrinos. American Journal of Modern Physics 5: 172-176.
15. Warber SL, Cornelio D, Straughn, J, Kile G (2004) Biofield energy healing from the inside. J Altern Complement Med 10: 1107-1113.
16. Hammerschlag R, Levin M, McCraty R, Bat N, Ives JA, Lutgendorf SK, Oschman JL (2015). Biofield physiology: A framework for an emerging discipline. Glob Adv Health Med 4: 35-41.
17. Rubik B, Muehsam D, Hammerschlag R, Jain S (2015) Biofield science and healing: History, terminology, and concepts. Glob Adv Health Med 4: 8-14.
18. Barnes PM, Bloom B, Nahin RL (2008) Complementary and alternative medicine use among adults and children: United States, 2007. Natl Health Stat Report 12: 1-23.
19. Trivedi MK, Patil S, Shettigar H, Bairwa K, Jana S (2015) Effect of biofield treatment on spectral properties of paracetamol and piroxicam. ChemSci J 6: 98.
20. Trivedi MK, Branton A, Trivedi D, Shettigar H, Bairwa K, Jana S (2015) Fourier transform infrared and ultraviolet-visible spectroscopic characterization of biofield treated salicylic acid and sparfloxacin. Nat Prod Chem Res 3: 186.
21. Trivedi MK, Patil S, Tallapragada RM (2013) Effect of biofield treatment on the physical and thermal characteristics of vanadium pentoxide powders. J Material Sci Eng S 11: 001.
22. Trivedi MK, Tallapragada RM, Branton A, Trivedi D, Nayak G, Latiyal O, Jana S (2015) Characterization of physical and structural properties of aluminum carbide powder: Impact of biofield treatment. J Aeronaut Aerospace Eng 4: 142.
23. Trivedi MK, Tallapragada RM, Branton A, Trivedi D, Nayak G, Latiyal O, Jana S (2015) The potential impact of biofield energy treatment on the atomic and physical properties of antimony tin oxide nanopowder. American Journal of Optics and Photonics 3: 123-128.
24. Trivedi MK, Branton A, Trivedi D, Nayak G, Plikerd WD, Surguy PL, Kock RJ, Piedad RB, Callas RP, Ansari SA, Barrett SL, Friedman S, Christie SL, Chen Liu S-M, Starling SE, Jones S, Allen SM, Wasmus SK, Benczik TA, Slade TC, Orban T, Vannes VL, Schlosser VM, Albino YSY, Panda P, Sethi KK, Jana S (2017). A systematic study of the biofield energy healing treatment on physicochemical, thermal, structural, and behavioral properties of magnesium gluconate. International Journal of Bioorganic Chemistry 2: 135-145.
25. Trivedi MK, Branton A, Trivedi D, Nayak G, Wellborn BD, Smith DL, Koster DA, Patric E, Singh J, Vagt KS, Callas KJ, Panda P, Sethi KK, Jana S (2017) Characterization of physicochemical, thermal, structural, and behavioral properties of magnesium gluconate after treatment with the energy of consciousness. International Journal of Pharmacy and Chemistry 3: 1-12.
26. Trivedi MK, Branton A, Trivedi D, Nayak G, Mondal SC, Jana S (2015) Evaluation of biochemical marker - Glutathione and DNA fingerprinting of biofield energy treated *Oryza sativa*. American Journal of BioScience 3: 243-248.
27. Trivedi MK, Branton A, Trivedi D, Nayak G, Gangwar M, Jana S (2016) Molecular analysis of biofield treated eggplant and watermelon crops. Adv Crop Sci Tech 4: 208.
28. Trivedi MK, Branton A, Trivedi D, Nayak G, Mondal

SC, Jana S (2015) Effect of biofield treated energized water on the growth and health status in chicken (*Gallus gallus domesticus*). Poult Fish Wildl Sci 3: 140.

29. Kinney JP, Trivedi MK, Branton A, Trivedi D, Nayak G, Mondal SC, Jana S (2017) Overall skin health potential of the biofield energy healing based herbomineral formulation using various skin parameters. American Journal of Life Sciences 5: 65-74.
30. Dodon J, Trivedi MK, Branton A, Trivedi D, Nayak G, Gangwar M, Jana S (2017) The study of biofield energy treatment based herbomineral formulation in skin health and function. American Journal of BioScience. 5: 42-53.
31. Trivedi MK, Branton A, Trivedi D, Nayak G, Lee AC, Hancharuk A, Sand CM, Schnitzer DJ, Thanasi R, Meagher EM, Pyka FA, Gerber GR, Stromsnas JC, Shapiro JM, Streicher LN, Hachfeld LM, Hornung MC, Rowe PM, Henderson SJ, Benson SM, Holmlund ST, Salters SP, Panda P, Jana S (2017) A comprehensive analytical evaluation of the Trivedi Effect® - Energy of consciousness healing treatment on the physical, structural, and thermal properties of zinc chloride. American Journal of Applied Chemistry 5: 7-18.
32. Trivedi MK, Branton A, Trivedi D, Nayak G, Plikerd WD, Surguy PL, Kock RJ, Piedad RB, Callas RP, Ansari SA, Barrett SL, Friedman S, Christie SL, Chen Liu S-M, Starling SE, Jones S, Allen SM, Wasmus SK, Benczik TA, Slade TC, Orban T, Vannes VL, Schlosser VM, Albino YSY, Panda P, Sethi KK, Jana S (2017). A systematic study of the biofield energy healing treatment on physicochemical, thermal, structural, and behavioral properties of iron sulphate. International Journal of Bioorganic Chemistry 2: 135-145.
33. Langford JI, Wilson AJC (1978) Scherrer after sixty years: A survey and some new results in the determination of crystallite size. J Appl Cryst 11: 102-113.
34. Inoue M, Hirasawa I (2013) The relationship between crystal morphology and XRD peak intensity on $CaSO_4.2H_2O$. J Crystal Growth 380: 169-175.
35. Raza K, Kumar P, Ratan S, Malik R, Arora S (2014) Polymorphism: The phenomenon affecting the performance of drugs. SOJ Pharm Pharm Sci 1: 10.
36. Thiruvengadam E, Vellaisamy G (2014) Polymorphism in pharmaceutical ingredients a review. World Journal of Pharmacy and Pharmaceutical Sciences 3: 621-633.
37. Blagden N, de Matas M, Gavan PT, York P (2007) Crystal engineering of active pharmaceutical ingredients to improve solubility and dissolution rates. Adv Drug Deliv Rev 59: 617-630.
38. Trivedi MK, Patil S, Tallapragada RM (2014) Atomic, crystalline and powder characteristics of treated zirconia and silica powders. J Material Sci Eng 3: 144.
39. Sun J, Wang F, Sui Y, She Z, Zhai W, Wang C, Deng Y (2012) Effect of particle size on solubility, dissolution rate, and oral bioavailability: Evaluation using coenzyme Q10 as naked nanocrystals. Int J Nanomedicine 7: 5733-5744.
40. Buckton G, Beezer AE (1992) The relationship between particle size and solubility. Int J Pharmaceutics 82: R7-R10.
41. Bonn D, Eggers J, Indekeu J, Meunier J, Rolley E (2009) Wetting and spreading. Rev Mod Phys 81: 739.
42. Moore J (2010) Chemistry: The molecular science (4^{th} edn) Brooks Cole.
43. Bajaj S, Singla D, Sakhuja N (2012) Stability testing of pharmaceutical products. J App Pharm Sci 2: 129-138.
44. Pavia DL, Lampman GM, Kriz GS (2001) Introduction to spectroscopy. (3^{rd} edn), Thomson learning, Singapore.
45. Stuart BH (2004) Infrared spectroscopy: Fundamentals and applications in Analytical Techniques in the Sciences. John Wiley & Sons Ltd., Chichester, UK.